

# Manipulation of Entangled Photon Pairs in Sandwich Valley Photonic Crystals

Zhen Jiang, Chaoliang Xi, Chun Jiang\*, Guangqiang He\*

State Key Laboratory of Advanced Optical Communication Systems and Networks, Department of Electronic Engineering, Shanghai Jiao Tong University, Shanghai 200240, China

\*Corresponding authors: cjiang@sjtu.edu.cn, gghe@sjtu.edu.cn

**Abstract:** We propose a sandwich valley photonic crystal implementing the generation and topological transport of continuous frequency entangled biphotons. These extended valley kink states propagating in the sandwich domain show more tolerance for disorders. © 2023 The Author(s)

## 1. Introduction

Topological edge states provide a practicable way to conduct the topological transport of quantum states. The topological protection of topological edge states brings many applicable approaches, including topological quantum emitters[1], topological quantum interference[2], and topological biphoton states[3-4].

It is noted that topological edge states are expected to be generated at the interface between trivial and nontrivial topological regions. These topological edge states show nonnegligible robustness against sharp bends, however, due to the limited area of the topological interface, the topological protection can be broken with large structure imperfections [5]. Here we propose a sandwich valley photonic crystal (VPC) producing two edge states, including a large-area topological edge state localized in the sandwich domain, and a normal topological edge state localized at the outer interface. Due to the four-wave mixing (FWM) process excited by the pump, the signal and idler photons propagating along the sandwich domain are theoretically proved to be continuous frequency entangled. This proposal may stimulate a potential interest in quantum properties in a large-area topological waveguide.

## 2. Extended valley kink states

Compared with traditional valley kink states generated at the topological interface, the extended valley kink states propagating in the sandwich domain show more tolerance for disorders. A scheme of sandwich VPCs based on the silicon slab is depicted in Fig. 1(a), which is composed of three different VPCs, referred to as the VPC<sub>1</sub>, primary valley photonic crystal (PVPC), and VPC<sub>2</sub>. The supercell of the topological VPC (Fig. 1(b)) reveals that there exist three molecular layers of PVPCs cells in the sandwich region. Corresponding unit cells of VPCs are illustrated in Fig. 1(c), where the lattice constant of VPCs is  $a$ , the sizes of triangle nanoholes are  $d_1$  and  $d_2$  respectively.

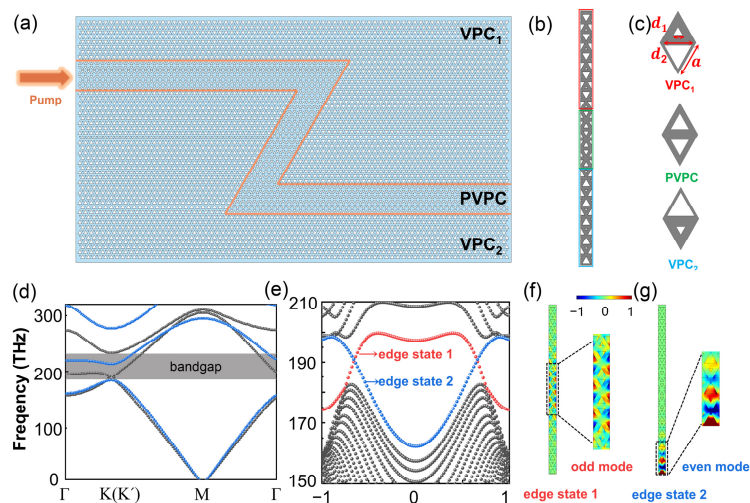


Fig. 1. (a) A scheme of topological sandwich VPCs. (b) A supercell of sandwich VPCs with three molecular layers of PVPCs. (c) Unit cells of the VPC<sub>1</sub> ( $d_1 = 0.25a$ ,  $d_2 = 0.75a$ ), PVPC ( $d_1 = d_2 = 0.5a$ ), and VPC<sub>2</sub> ( $d_1 = 0.75a$ ,  $d_2 = 0.25a$ ), where  $a = 360$  nm. (d) Calculated band structure of the primary (grey dots) and perturbed (blue dots) unit cells. (e) Dispersion relation of the supercell composed of three types of VPCs. Field profiles of (f) edge state 1 and (g) edge state 2 at the frequency of 196.6 THz.

For a PVPC unit cell ( $d_1 = d_2 = 0.5a$ ), the perfect  $C_6$  lattice symmetry leads to a degenerate Dirac cone (corresponding to K and  $K'$  valleys), as shown by the gray dots in Fig. 1(d). when the lattice symmetry is perturbed ( $d_1 \neq d_2$ ), the degradation of Dirac cones gives rise to the bandgap. The dispersion relation of the supercell composed of three types of VPCs is shown in Fig. 1(e). Remarkably, there exist two edge states localized in the topological bandgap, which are depicted by red and blue dots respectively. The field profiles of these two edge states at the frequency of 196.6 THz are plotted in Fig. 1(f) and (g). These two states are identified by a large-area topological edge state localized in the sandwich domain, and a normal topological edge state localized at the outer interface. For the case of edge state 1, the electric field of this mode fills the entire sandwich domain, showing considerable light confinement. The eigenmodal fields reveal that they have opposite mode distributions, referred to as odd and even modes.

### 3. Quantum entanglement of photon pairs

To get insight into the robustness of extended valley kink states, we construct a sandwich VPC with a “Z” shaped domain, and 12 nanoholes in this sandwich region are removed. The simulated electric field profile of extended valley kink states is shown in Fig. 2(a). The result reveals that such large-area kink states are insensitive to sharp bends and disorders.

With the injection of the pump, the degenerate FWM process leads to the generation of signal and idler photons. Two equations should be satisfied for the FWM process, that is,  $2\hbar\omega_p = \hbar\omega_s + \hbar\omega_i$  and  $2k_p = k_s + k_i$ , where  $\omega$  and  $k$  are the angular frequency and wavevector. The biphoton state  $|\Psi\rangle$  of this FWM process is given by  $|\Psi\rangle = \iint d\omega_s d\omega_i \mathcal{A}(\omega_s, \omega_i) \hat{a}^\dagger_{\omega_s} \hat{a}^\dagger_{\omega_i} |0\rangle$ , where  $\mathcal{A}(\omega_s, \omega_i)$  is the joint spectral amplitude (JSA) of biphoton states,  $\hat{a}^\dagger_{\omega_s}$  is the creation operator. When the JSA of biphoton states cannot be factorized into the formation of  $\omega_s$  and  $\omega_i$ , the signal and idler photons are entangled. The calculated JSA of the biphoton state of extended valley kink states is plotted in Fig. 2(b), showing that the biphotons are strongly anticorrelated. Using the Schmidt decomposition method to estimate the entanglement between signal and idler photons. The values of normalized Schmit coefficient  $\lambda_n$  are shown in Fig. 2(c), the number of nonzero Schmit coefficient  $\lambda_n$  is greater than 1, meaning that the biphotons generated via the FWM process in the sandwich region are continuous frequency entangled. And the inset shows that the convergency value of the entropy of entanglement is 5.425, which also clarifies the entanglement between signal and idler photons. It worth mentioning that the biphoton state propagating in the sandwich region is topologically protected. Notably, this biphoton state generated in the sandwich region are born to be topologically protected.

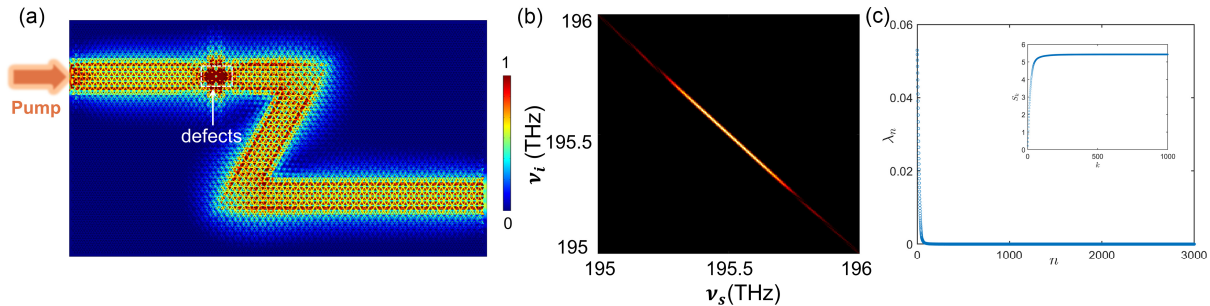


Fig. 2. (a) Simulated electric field profile of extended valley kink states. (b) JSA of photon pairs generated from the FWM process in topological PCs. (c) Normalized Schmidt coefficient, the inset denotes the entropy of entanglement.

### 4. Conclusion

Here, we propose a sandwich VPC supporting the generation and topological transport of continuous frequency entangled biphotons. The result implies that the entangled photon pairs are robust against sharp bends and disorders. This proposal may give inspiration for large-area transport of quantum states.

The authors acknowledge the support from the Key-Area Research and Development Program of Guangdong Province (2018B030325002), the National Natural Science Foundation of China (62075129/ 61975119), and the SJTU Pinghu Institute of Intelligent Optoelectronics (2022SPIOE204).

### References

- [1] S. Barik, "A topological quantum optics interface," *Science* 359, 666-668 (2018).
- [2] S. Mittal, "Tunable quantum interference using a topological source of indistinguishable photon pairs," *Nat. Photon.* 15, 542-548 (2021).
- [3] Z. Jiang, "Topological protection of continuous frequency entangled biphoton states," *Nanophotonics* 10, 4019-4026 (2021).
- [4] Z. Jiang, "Topologically protected energy-time entangled biphoton states in photonic crystals," *J. Phys. D: Appl. Phys.* 55, 315104 (2022).
- [5] J Q. Wang, "Extended topological valley-locked surface acoustic waves," *Nat. Commun.* 13, 1324 (2022).